

Losartan, an AT1 Antagonist, Prevents Aortic Aneurysm in a Mouse Model of Marfan Syndrome

Jennifer P. Habashi,^{1*} Daniel P. Judge,^{2*} Tammy M. Holm,¹ Ronald D. Cohn,¹ Bart L. Loeys,¹ Timothy K. Cooper,^{1,3} Loretha Myers,¹ Erin C. Klein,¹ Guosheng Liu,³ Carla Calvi,² Megan Podowski,² Enid R. Neptune,² Marc K. Halushka,⁴ Djahida Bedja,³ Kathleen Gabrielson,³ Daniel B. Rifkin,⁵ Luca Carta,⁶ Francesco Ramirez,⁶ David L. Huso,³ Harry C. Dietz^{1,2,†}

Aortic aneurysm and dissection are manifestations of Marfan syndrome (MFS), a disorder caused by mutations in the gene that encodes fibrillin-1. Selected manifestations of MFS reflect excessive signaling by the transforming growth factor- β (TGF- β) family of cytokines. We show that aortic aneurysm in a mouse model of MFS is associated with increased TGF- β signaling and can be prevented by TGF- β antagonists such as TGF- β -neutralizing antibody or the angiotensin II type 1 receptor (AT1) blocker, losartan. AT1 antagonism also partially reversed noncardiovascular manifestations of MFS, including impaired alveolar septation. These data suggest that losartan, a drug already in clinical use for hypertension, merits investigation as a therapeutic strategy for patients with MFS and has the potential to prevent the major life-threatening manifestation of this disorder.

MFS is a systemic disorder of connective tissue caused by mutations in *FBN1*, the gene encoding fibrillin-1 (1). As a principal component of the extracellular matrix microfibril (2, 3), fibrillin-1 was initially thought to play primarily a structural role in connective tissue. Several lines of evidence support an additional role as a regulator of the cytokine TGF- β (4, 5). Mice homozygous for a hypomorphic *Fbn1* allele have impaired pulmonary alveolar septation associated with increased TGF- β signaling that can be prevented by perinatal administration of a polyclonal TGF- β neutralizing antibody (NAb) (5). Similarly, myxomatous thickening of the cardiac atrioventricular valves in mice harboring a *Fbn1* missense mutation is attenuated by perinatal systemic administration of TGF- β NAb (6).

We sought to determine the role of TGF- β in MFS-associated aortic aneurysm, which is the major life-threatening manifestation of this condition. We studied mice heterozygous for an *Fbn1* allele encoding a cysteine substitution, Cys¹⁰³⁹ \rightarrow Gly (C1039G), in an epidermal growth factor–like domain of fibrillin-1 (*Fbn1*^{C1039G/+}) (6–8), which is the most common class of mutation causing MFS. The

aortic root in *Fbn1*^{C1039G/+} mice undergoes progressive dilatation, evident as early as 2 weeks of age. By 7 weeks of age, the aortic root in the mutant mice is larger than that in wild-type mice (1.82 \pm 0.14 mm versus 1.59 \pm 0.11 mm, respectively; $P < 0.05$). This size difference becomes more pronounced with age (aortic root at 8 months, 2.47 \pm 0.33 mm versus 1.82 \pm 0.11 mm; $P < 0.0001$).

Histologic analysis of 14-week-old *Fbn1*^{C1039G/+} mice revealed aberrant thickening of the aortic media with fragmentation and disarray of elastic fibers (fig. S1). In addition, *Fbn1*^{C1039G/+} mice showed increased collagen deposition, which is an indirect marker of increased TGF- β signaling (fig. S1) (9, 10). Phosphorylation and subsequent nuclear translocation of Smad2 (pSmad2), which are induced by TGF- β signaling (11), are markedly increased in the aortic media of *Fbn1*^{C1039G/+} mice relative to wild-type mice (fig. S1). Similar changes have been observed in aortic samples derived from patients with MFS (12).

To investigate whether excessive TGF- β signaling plays a causal role in progressive aortic root enlargement, we treated mice postnatally with TGF- β NAb after the establishment of aortic root aneurysm (Fig. 1). Treatment by intraperitoneal injection was begun at 7 weeks of age and continued for 8 weeks. The *Fbn1*^{C1039G/+} mice received low-dose TGF- β NAb (1 mg/kg body weight; Fig. 1, C and G), high-dose TGF- β NAb (10 mg/kg; Fig. 1, D and H), or placebo (10 mg/kg rabbit IgG; Fig. 1, B and F) every 2 weeks. Histologic analyses revealed reduced elastic fiber fragmentation and reduced TGF- β signaling in the aortic media of TGF- β NAb-treated mice relative to the placebo group (Fig. 1, A to H). In humans with MFS, the diameter and rate of

enlargement of the aortic root are directly proportional to the risk of life-threatening aortic dissection (13). Echocardiograms revealed that the aortic root diameter at baseline in the wild-type mice (1.57 \pm 0.05 mm) was smaller than that in the three *Fbn1*^{C1039G/+} treatment arms [placebo, 1.75 \pm 0.15 mm; NAb (10 mg/kg), 1.80 \pm 0.11 mm; NAb (1 mg/kg), 1.86 \pm 0.15 mm; $P < 0.0001$ for each treatment arm relative to wild type]. There was no difference in the growth rate of the aortic root, as assessed by echocardiograms performed after 8 weeks of treatment, between wild-type mice and either of the TGF- β NAb treatment groups ($P = 0.11$). In contrast, the aortic root growth rate in the placebo-treated mice was greater than that in either wild-type ($P < 0.0001$) or NAb-treated mice ($P < 0.03$, Fig. 1I). After 8 weeks, aortic wall thickness in NAb-treated *Fbn1*^{C1039G/+} mice was indistinguishable from that in untreated wild-type mice ($P = 0.91$) and less than that in the placebo group ($P < 0.01$, Fig. 1J). Aortic wall architecture was disrupted in *Fbn1*^{C1039G/+} mice relative to wild-type mice ($P < 0.0001$) but improved in mutant mice treated with NAb ($P < 0.001$, Fig. 1K). These data show that excessive TGF- β signaling contributes to the formation of aortic aneurysm in a mouse model of MFS, and that TGF- β antagonism represents a productive treatment strategy.

We became interested in losartan, an angiotensin II type 1 receptor (AT1) antagonist, not only because it lowers blood pressure—a desirable effect in patients with aortic aneurysm—but also because it leads to antagonism of TGF- β in animal models of chronic renal insufficiency and cardiomyopathy (14, 15). Using a prenatal administration protocol in our mouse model, we compared the efficacy of losartan to that of propranolol, which is representative of β -adrenergic blocking agents widely used in patients with MFS to slow the rate of aortic growth (16). The doses of losartan and propranolol were titrated to achieve comparable hemodynamic effects in vivo, including a 15 to 20% decrease in heart rate and a 10 to 20% decrease in blood pressure in both groups.

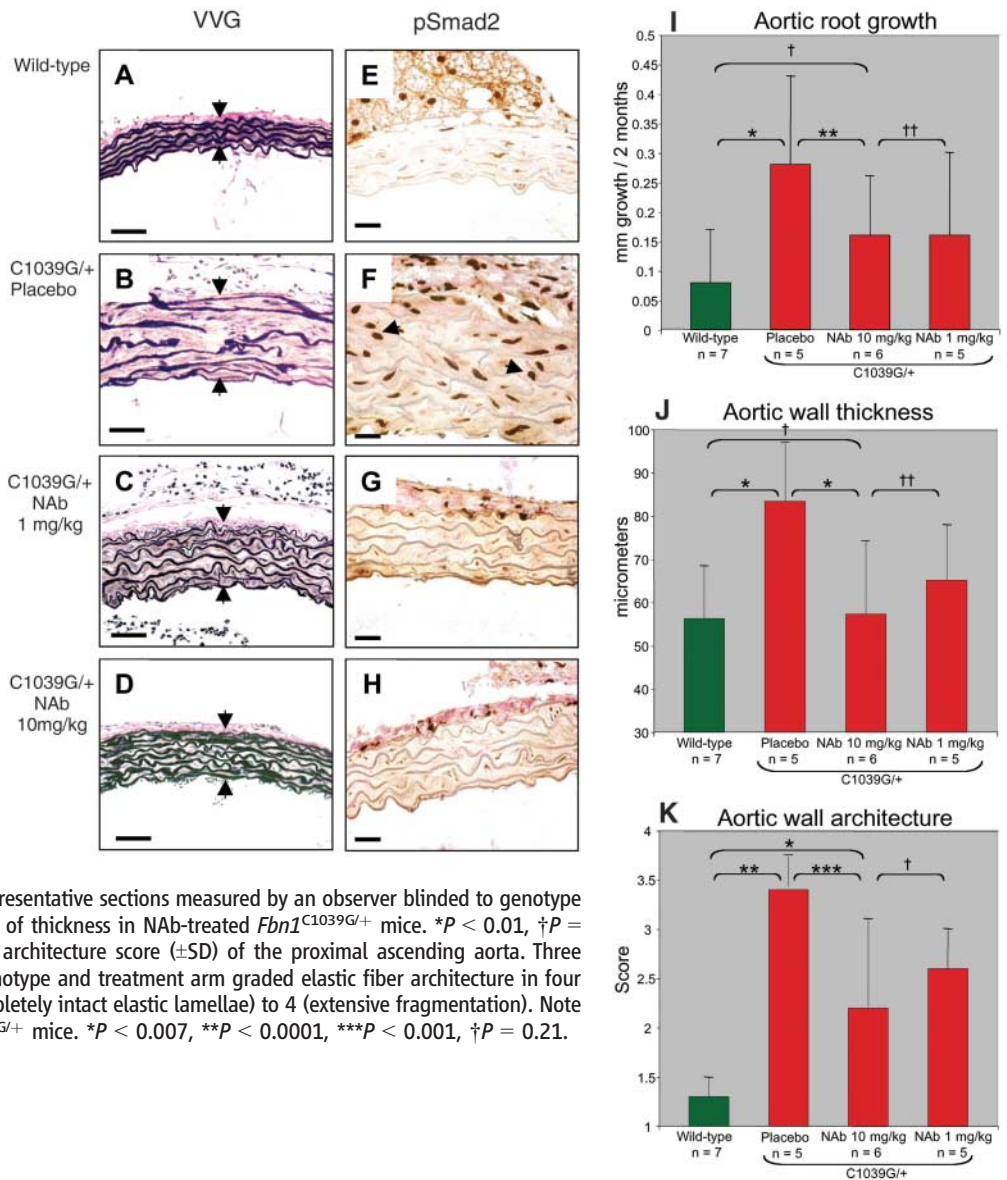
Pregnant *Fbn1*^{C1039G/+} mice received losartan (0.6 g/liter), propranolol (0.5 g/liter), or placebo in their drinking water, beginning at 2 weeks of gestation. Treatment of the mothers continued throughout lactation and was maintained in the pups after weaning. Mice were killed at 10 months of age. Elastic fiber fragmentation was observed in both placebo- and propranolol-treated mice, but not in losartan-treated mice (Fig. 2, A to D). The average aortic wall thickness for untreated wild-type animals was smaller than that in placebo-treated *Fbn1*^{C1039G/+} mice ($P < 0.0001$) but was indistinguishable from that in losartan-treated *Fbn1*^{C1039G/+} mice ($P = 0.24$, Fig. 2E). Aortic wall thickness in the propranolol-treated mice was indistinguishable from that in the placebo

¹Howard Hughes Medical Institute and Department of Pediatrics, ²Department of Medicine, ³Department of Molecular and Comparative Pathobiology, ⁴Department of Pathology, Johns Hopkins University School of Medicine, Baltimore, MD 21205, USA. ⁵Departments of Cell Biology and Medicine, New York University School of Medicine, New York, NY 10016, USA. ⁶Child Health Institute of New Jersey, University of Medicine and Dentistry of New Jersey—Robert Wood Johnson Medical School, New Brunswick, NJ 08903, USA.

*These authors contributed equally to this work.

†To whom correspondence should be addressed. E-mail: hdietz@jhmi.edu

Fig. 1. Postnatal treatment with TGF- β NAb. **(A to H)** Characterization of the ascending aorta in untreated wild-type mice **(A)** and **(E)** and *Fbn1*^{C1039G/+} mice treated with placebo **(B)** and **(F)**, 1 mg/kg TGF- β NAb **(C)** and **(G)**, and 10 mg/kg TGF- β NAb **(D)** and **(H)**. In **(A)** to **(D)**, Verhoeff's-van Gieson (VVG) stain reveals diffuse disruption of elastic fiber architecture and thickening of the aortic media (delineated by arrows) in placebo-treated *Fbn1*^{C1039G/+} mice **(B)** relative to the normal elastic fiber architecture observed in wild-type mice **(A)**. Improvement in both parameters is seen in NAb-treated *Fbn1*^{C1039G/+} mice **(C)** and **(D)**. Scale bars, 50 μ m. In **(E)** to **(H)**, immunohistochemistry (IH) reveals nuclear pSmad2, a marker for TGF- β signaling (arrows indicate representative positive nuclei). Increased pSmad2 is observed in the placebo-treated *Fbn1*^{C1039G/+} mice **(F)** relative to wild-type mice **(E)**. Normalized pSmad2 staining is observed in the NAb-treated *Fbn1*^{C1039G/+} mice **(G)** and **(H)**. Scale bars, 50 μ m. **(I)** Average aortic root growth (\pm SD) measured by echocardiogram over the 2-month treatment period. Note the reduced rate of growth in the NAb-treated mice relative to the placebo-treated *Fbn1*^{C1039G/+} mice. **P* < 0.0001, ***P* < 0.03, †*P* = 0.11, ††*P* = 1.0. **(J)** Average thickness (\pm SD) of the proximal ascending aortic media of four representative sections measured by an observer blinded to genotype and treatment arm. Note full normalization of thickness in NAb-treated *Fbn1*^{C1039G/+} mice. **P* < 0.01, †*P* = 0.91, ††*P* = 0.38. **(K)** Average aortic wall architecture score (\pm SD) of the proximal ascending aorta. Three separate observers who were blinded to genotype and treatment arm graded elastic fiber architecture in four representative areas on a scale from 1 (completely intact elastic lamellae) to 4 (extensive fragmentation). Note the improvement in NAb-treated *Fbn1*^{C1039G/+} mice. **P* < 0.007, ***P* < 0.0001, ****P* < 0.001, †*P* = 0.21.



group (*P* = 0.19). Likewise, aortic wall architecture was normalized in losartan-treated *Fbn1*^{C1039G/+} animals relative to the placebo group (*P* < 0.0001) but was not influenced by propranolol (*P* = 0.16, Fig. 2F). There was marked aortic dilatation in the placebo- and propranolol-treated mutant mice, whereas the losartan-treated mutant mice were indistinguishable from wild-type littermates (fig. S2).

Because MFS is typically diagnosed after birth and because the use of AT1 antagonists is contraindicated during pregnancy (17), we investigated whether losartan could attenuate or prevent abnormal aortic root growth if treatment were initiated postnatally, after the establishment of aortic aneurysms. At 7 weeks of age, after echocardiographic documentation of aneurysm (fig. S3), *Fbn1*^{C1039G/+} mice received placebo, propranolol (0.5 g/liter), or losartan (0.6 g/liter) in their drinking water. Baseline echocardiograms revealed no differ-

ences in aortic root size between any of the treatment groups for *Fbn1*^{C1039G/+} mice (placebo 1.83 \pm 0.11 mm, propranolol 1.92 \pm 0.27 mm, losartan 1.84 \pm 0.08 mm, respectively; *P* = 0.5). However, before treatment, the aortic diameter in *Fbn1*^{C1039G/+} mice was always greater than in untreated wild-type mice (1.59 \pm 0.11 mm; *P* < 0.002) (fig. S3).

Three independent aortic root measurements were obtained for each mouse every 2 months during the 6 months of treatment. Mice were killed at 8 months of age. In contrast to propranolol or placebo, losartan treatment prevented elastic fiber fragmentation (Fig. 3, A to D) and blunted TGF- β signaling in the aortic media, as evidenced by reduced nuclear accumulation of pSmad2 (Fig. 3, E to H). The aortic root growth rate over this period was less in the wild-type mice than in the placebo-treated *Fbn1*^{C1039G/+} mice (*P* < 0.0001, Fig. 3I). Although the propranolol-treated *Fbn1*^{C1039G/+}

mice did show a slower rate of aortic root growth than did placebo-treated animals (*P* < 0.001), this growth rate remained greater than that in untreated wild-type mice (*P* < 0.04). In contrast, the aortic root growth rate in losartan-treated *Fbn1*^{C1039G/+} mice was indistinguishable from that in the wild-type group (*P* = 0.55, Fig. 3I). Furthermore, the absolute diameter of the aortic root at the end of treatment was similar in the losartan-treated *Fbn1*^{C1039G/+} mice and untreated wild-type littermates (*P* = 0.32; fig. S3). Propranolol had no discernable effect on either aortic wall thickness or elastic fiber architecture when compared to placebo; hence, its beneficial effect is limited to slowing the rate of growth of the aortic root. In contrast, losartan-treated *Fbn1*^{C1039G/+} mice showed improvement in all three parameters compared to placebo-treated mice, with full normalization relative to wild-type mice (Fig. 3, I to K). We conclude that

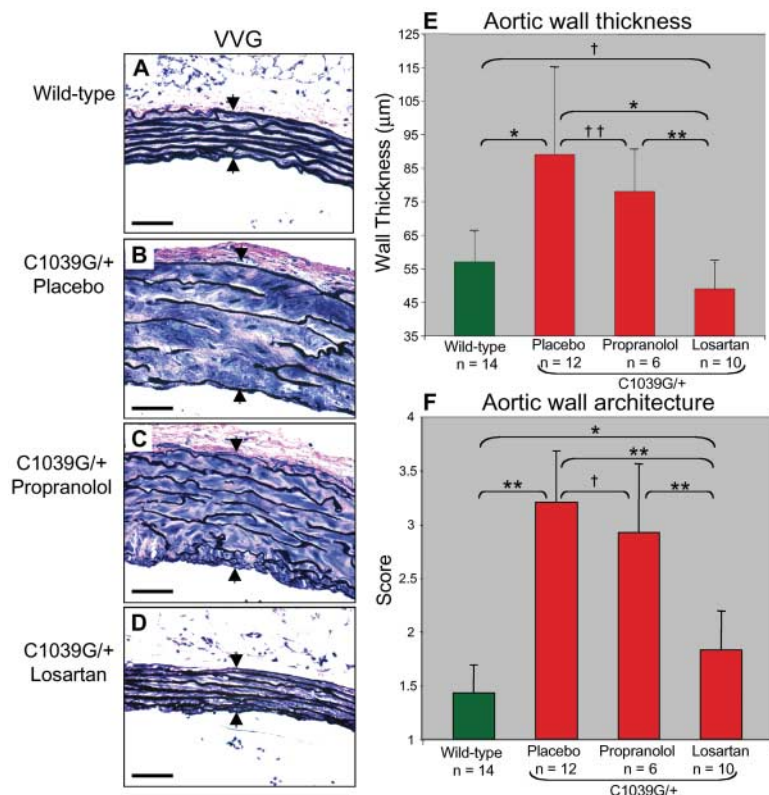


Fig. 2. Prenatal treatment with losartan and propranolol. (A to D) VVG staining highlights intact elastic fiber architecture and normal ascending aortic wall thickness (arrows) in wild-type mice (A) and losartan-treated *Fbn1*^{C1039G/+} mice (D). Marked elastic fiber disruption and wall thickening is apparent in the placebo- and propranolol-treated *Fbn1*^{C1039G/+} mice [(B) and (C).] Scale bars, 40 µm. (E) Average aortic wall thickness (±SD) after 10 months of treatment. Note full normalization of wall thickness in losartan-treated *Fbn1*^{C1039G/+} mice relative to mice that received placebo or propranolol treatment. **P* < 0.0001, ***P* < 0.002, †*P* = 0.24, ††*P* = 0.19. (F) Average aortic wall architecture score (±SD) after treatment. Note the improvement in losartan-treated *Fbn1*^{C1039G/+} mice. **P* < 0.02, ***P* < 0.0001, †*P* = 0.16.

β-adrenergic blockade with propranolol diminishes aortic growth rate in this model of MFS but does not prevent progressive deterioration of aortic wall architecture or ongoing abnormal aortic dilatation. In contrast, AT1 blockade with losartan appears to achieve full correction of the phenotypic abnormalities in the aortic wall of *Fbn1*^{C1039G/+} mice.

In a previous study, we showed that a different strain of mice homozygous for hypomorphic *Fbn1* alleles showed widening of the distal airspace due to failure of alveolar septation (5). This abnormality correlated with increased TGF-β signaling and was prevented by prenatal administration of TGF-β NAb (5). To determine whether losartan can improve this lung phenotype when administered postnatally—a matter of specific relevance to patients with MFS—we treated *Fbn1*^{C1039G/+} mice with losartan beginning at 7 weeks of age. After 6 months of treatment, placebo-treated *Fbn1*^{C1039G/+} mice showed widening of the distal airspace due to impaired alveolar septation (mean linear intercept 84.3 ± 15 µm) relative to wild-type placebo-treated mice (mean linear intercept 41.3 ± 5 µm, *P* < 0.001; Fig. 4).

Losartan-treated *Fbn1*^{C1039G/+} mice showed a reduction in distal airspace caliber relative to placebo-treated *Fbn1*^{C1039G/+} animals (mean linear intercept 53.9 ± 12 µm, *P* < 0.001; Fig. 4).

AT1 antagonism might achieve superior protection over β-adrenergic blocking agents by virtue of increased blunting of the hemodynamic stress that is imposed on a structurally deficient aortic wall, as opposed to a mechanism relevant to TGF-β signaling or other molecular pathogenetic events. Four lines of evidence argue against this hypothesis. First, the doses of losartan and propranolol were titrated to achieve comparable hemodynamic effects. Second, isolated antagonism of TGF-β signaling with NAb provides similar protection. Third, analysis of pSmad2 nuclear staining revealed that losartan antagonizes TGF-β signaling in the aortic wall of *Fbn1*^{C1039G/+} mice, an event seen in NAb-treated mice but not in propranolol-treated mice (Fig. 3, G and H). Fourth, we demonstrate here that losartan can improve disease manifestations in the lungs (Fig. 4), an event that cannot plausibly relate to improved hemodynamics.

The mechanism by which AT1 blockade antagonizes TGF-β signaling remains to be fully elucidated. Signaling through the AT1 receptor increases the expression of TGF-β ligands and receptors and also induces the expression of thrombospondin-1, a potent activator of TGF-β (18–21). In the vessel wall, AT1 signaling stimulates proliferation of vascular smooth muscle cells (VSMCs) and vessel wall fibrosis (22), although this may be context-dependent. In avian systems, neural crest- and mesoderm-derived VSMCs (N- and M-VSMCs, respectively) respond differently to TGF-β1, with cellular proliferation and fibrosis seen in the former and growth inhibition seen in the latter (23, 24). This differential response may explain the particular predisposition of the root of the aorta—a vascular segment enriched for N-VSMCs—to undergo dilatation and dissection in MFS. The pulmonary artery root is also enriched for N-VSMCs and routinely shows dilatation in MFS despite the reduced pressure in the pulmonary circulation (25).

Given that signaling through the angiotensin II type 2 receptor (AT2) antagonizes many of the effects that are promoted by AT1 signaling (26), specific AT1 antagonism may be preferable to the dual AT1/AT2 blockade achieved with angiotensin converting enzyme (ACE) inhibitors. Consistent with this hypothesis, Daugherty and colleagues found that the formation of angiotensin II-induced abdominal aortic aneurysms could be prevented in apoE^{-/-} mice by treatment with AT1 antagonists but was accelerated in both frequency and severity upon treatment with a selective AT2 blocker (27). Nagashima and colleagues observed increased apoptosis in vessel wall explants and cultured VSMCs from individuals with MFS, and they showed that AT2 but not AT1 blockade reduced this effect (28, 29). These samples were derived from aneurysms in the 7- to 9-cm range, far beyond the current threshold for aortic root surgery. In our mouse model, we have not detected enhanced apoptosis in early and intermediate stages of aortic aneurysm (fig. S4). Angiotensin II also stimulates Smad2-dependent signaling and fibrosis in VSMCs in a TGF-β-independent manner, and this effect can be prevented by selective AT1 blockade (30). Thus, although TGF-β ligand-dependent signaling appears critical to the pathogenesis of aortic aneurysm in MFS, antagonism of a parallel pSmad2-mediated signaling cascade may contribute to the protection afforded by losartan.

The demonstration of excess TGF-β signaling in the aortic wall of patients with other aortic aneurysm syndromes, including Loey-Dietz syndrome (caused by mutations in *TGFBR1* or *TGFBR2*) and arterial tortuosity syndrome (caused by mutations in *GLUT10*), suggests that losartan may be of broad relevance in the treatment of human vasculopathies (12, 31).

Losartan is currently in widespread clinical use for treatment of hypertension and prevention

Fig. 3. Postnatal treatment with losartan and propranolol. (A to H) VVG staining [(A) to (D)] and pSmad2 immunostaining [(E) to (H)] of aortic wall. Elastic lamellae are intact and aortic media is of normal thickness in the wild-type (A) and losartan-treated *Fbn1*^{C1039G/+} mice (D). Placebo- and propranolol-treated *Fbn1*^{C1039G/+} mice [(B) and (C)] have diffuse fragmentation of elastic fibers and thickening of the aortic media (arrows). Scale bars, 50 μ m. Nuclear pSmad2 staining is decreased in the aortic media of wild-type (E) and losartan-treated *Fbn1*^{C1039G/+} mice (H). Marked increase in nuclear staining for pSmad2 (representative positive cells denoted by arrowheads) is seen in the *Fbn1*^{C1039G/+} mice treated with placebo (F) and propranolol (G). Scale bars, 40 μ m. (I) Average aortic root growth (\pm SD) during the 6 months of treatment. Note that aortic root growth in *Fbn1*^{C1039G/+} mice treated with propranolol is less than that with placebo, yet remains greater than that seen in wild-type mice. Losartan treatment normalizes growth rate. **P* < 0.0001, ***P* < 0.001, ****P* < 0.02, †*P* = 0.55. (J) Average aortic wall thickness (\pm SD). Aortic wall thickness in losartan-treated *Fbn1*^{C1039G/+} mice is reduced relative to placebo- and propranolol-treated mice and is indistinguishable from that seen in wild-type mice. **P* < 0.002, ***P* < 0.0001, ****P* < 0.05, †*P* = 0.67, ††*P* = 0.17. (K) Average aortic wall architecture (\pm SD). Note full normalization achieved with losartan treatment. **P* < 0.002, ***P* < 0.0001, ****P* < 0.05, †*P* = 0.20, ††*P* = 0.47.

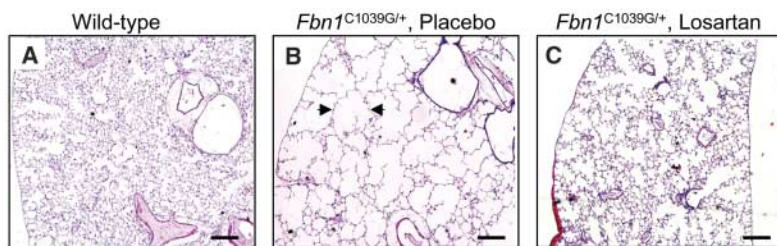
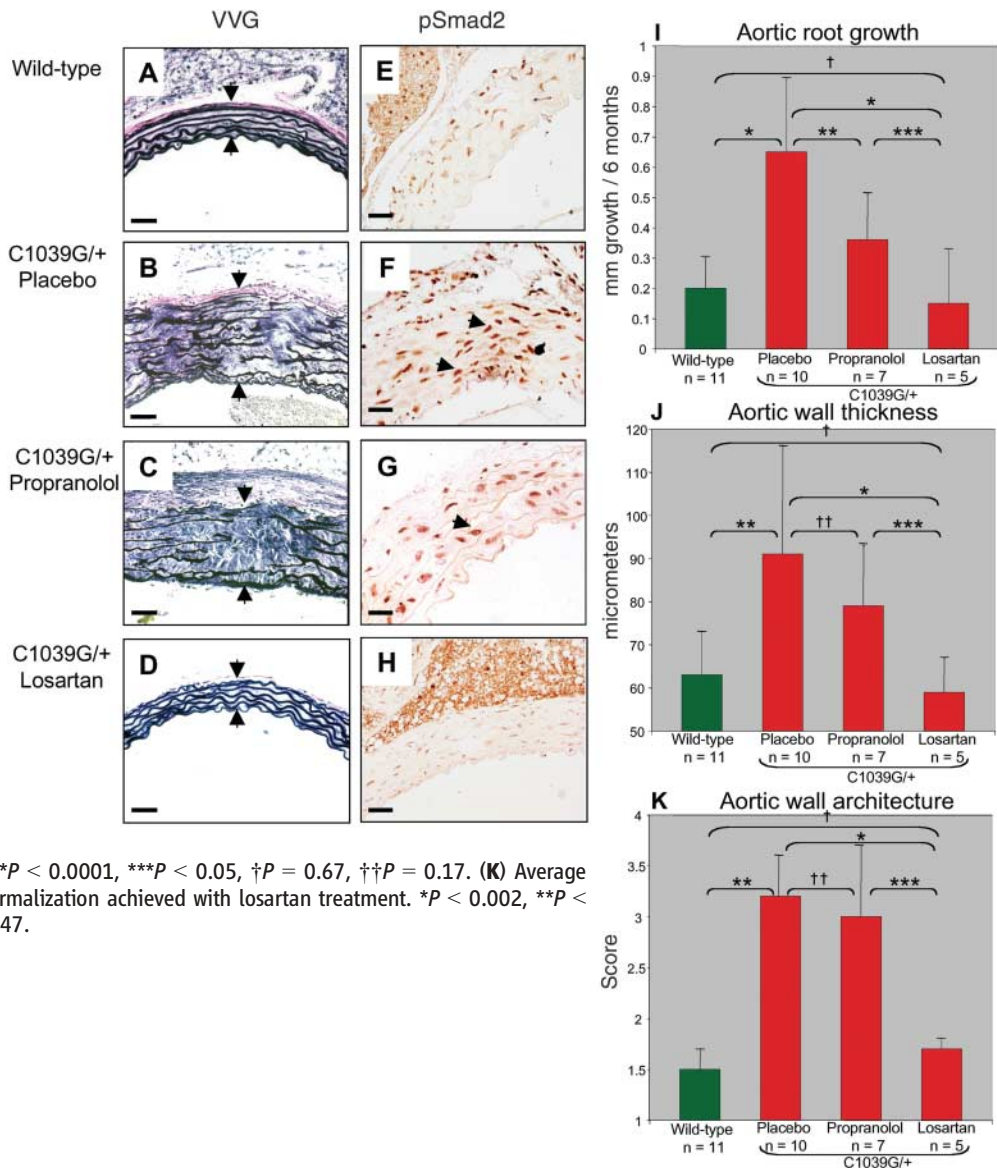
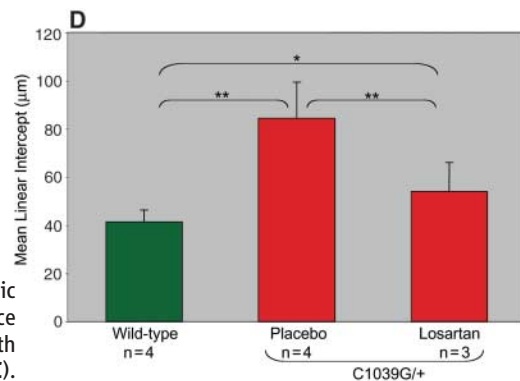


Fig. 4. Postnatal losartan treatment of lung disease in *Fbn1*^{C1039G/+} mice. Histologic analysis of lung in wild-type mice (A) shows normal airspace caliber. *Fbn1*^{C1039G/+} mice treated with placebo (B) show diffuse distal airspace widening (example delineated with arrows). Distal airspace caliber is reduced in *Fbn1*^{C1039G/+} mice treated with losartan (C). Scale bars, 500 μ m. (D) Average mean linear intercept, a marker of airspace caliber, is greater for placebo-treated *Fbn1*^{C1039G/+} mice than for untreated wild-type and losartan-treated *Fbn1*^{C1039G/+} mice. **P* < 0.01, ****P* < 0.001.



of strokes in both adults and children. Given its exceptional tolerance profile in all age groups, we conclude that a prospective clinical trial in patients with MFS is indicated. Furthermore, this

study is illustrative of the promise that enhanced identification of disease genes in the post-genome sequencing era will have a pronounced impact on medicine. Disease gene discovery is

but an obligate first step in the process of making animal models, interrogating pathogenesis, and deriving unanticipated disease mechanisms and rational treatment strategies.

References and Notes

1. H. C. Dietz *et al.*, *Nature* **352**, 337 (1991).
2. L. Y. Sakai, D. R. Keene, R. W. Glanville, H. P. Bachinger, *J. Biol. Chem.* **266**, 14763 (1991).
3. R. P. Visconti, J. L. Barth, F. W. Keeley, C. D. Little, *Matrix Biol.* **22**, 109 (2003).
4. Z. Isogai *et al.*, *J. Biol. Chem.* **278**, 2750 (2003).
5. E. R. Neptune *et al.*, *Nat. Genet.* **33**, 407 (2003).
6. C. M. Ng *et al.*, *J. Clin. Invest.* **114**, 1586 (2004).
7. D. P. Judge *et al.*, *J. Clin. Invest.* **114**, 172 (2004).
8. K. B. Jones *et al.*, *Spine* **30**, 291 (2005).
9. P. Rossi *et al.*, *Cell* **52**, 405 (1988).
10. W. Schlumberger, M. Thie, J. Rauterberg, H. Robenek, *Arterioscler. Thromb.* **11**, 1660 (1991).
11. C. H. Heldin, K. Miyazono, P. ten Dijke, *Nature* **390**, 465 (1997).
12. B. L. Loeys *et al.*, *Nat. Genet.* **37**, 275 (2005).
13. V. L. Gott *et al.*, *N. Engl. J. Med.* **340**, 1307 (1999).
14. P. Lavoie *et al.*, *J. Hypertens.* **23**, 1895 (2005).
15. D. S. Lim *et al.*, *Circulation* **103**, 789 (2001).
16. J. Shores, K. R. Berger, E. A. Murphy, R. E. Pyeritz, *N. Engl. J. Med.* **330**, 1335 (1994).
17. S. G. Spence *et al.*, *Teratology* **51**, 367 (1995).
18. A. D. Everett, A. Tufro-McReddie, A. Fisher, R. A. Gomez, *Hypertension* **23**, 587 (1994).
19. G. Wolf, F. N. Ziyadeh, R. A. Stahl, *J. Mol. Med.* **77**, 556 (1999).
20. N. Fukuda *et al.*, *Am. J. Hypertens.* **13**, 191 (2000).
21. T. Naito *et al.*, *Am. J. Physiol. Renal Physiol.* **286**, F278 (2004).
22. E. G. Nabel *et al.*, *Proc. Natl. Acad. Sci. U.S.A.* **90**, 10759 (1993).
23. P. F. Gadson Jr. *et al.*, *Exp. Cell Res.* **230**, 169 (1997).
24. S. Topouzis, M. W. Majesky, *Dev. Biol.* **178**, 430 (1996).
25. G. J. Nollen *et al.*, *Heart* **87**, 470 (2002).
26. E. S. Jones, M. J. Black, R. E. Widdop, *J. Mol. Cell. Cardiol.* **37**, 1023 (2004).
27. A. Daugherty, M. W. Manning, L. A. Cassis, *Br. J. Pharmacol.* **134**, 865 (2001).
28. H. Nagashima *et al.*, *Circulation* **104**, 1282 (2001).
29. J. Suzuki *et al.*, *Circulation* **106**, 847 (2002).
30. J. Rodriguez-Vita *et al.*, *Circulation* **111**, 2509 (2005).
31. P. J. Coucke *et al.*, *Nat. Genet.*, in press.
32. We thank K. Khan for expert technical assistance. Supported by the NIH (H.C.D., D.P.J., D.L.H., D.B.R., F.R.), the Smilow Center for Marfan Syndrome Research (H.C.D.), the National Marfan Foundation (H.C.D., D.P.J.), the Howard Hughes Medical Institute (H.C.D.), the Victor A. McKusick Endowment (H.C.D.), and the Dana and Albert "Cubby" Broccoli Center for Aortic Diseases (D.P.J.). All protocols for mouse treatment were approved by the Animal Care and Use Committee of the Johns Hopkins University School of Medicine.

Supporting Online Material

www.sciencemag.org/cgi/content/full/312/5770/117/DC1

Materials and Methods

Figs. S1 to S4

References

23 December 2005; accepted 2 March 2006

10.1126/science.1124287

This copy is for your personal, non-commercial use only.

If you wish to distribute this article to others, you can order high-quality copies for your colleagues, clients, or customers by [clicking here](#).

Permission to republish or repurpose articles or portions of articles can be obtained by following the guidelines [here](#).

The following resources related to this article are available online at www.sciencemag.org (this information is current as of March 13, 2015):

Updated information and services, including high-resolution figures, can be found in the online version of this article at:

<http://www.sciencemag.org/content/312/5770/117.full.html>

Supporting Online Material can be found at:

<http://www.sciencemag.org/content/suppl/2006/04/05/312.5770.117.DC1.html>

A list of selected additional articles on the Science Web sites **related to this article** can be found at:

<http://www.sciencemag.org/content/312/5770/117.full.html#related>

This article **cites 30 articles**, 11 of which can be accessed free:

<http://www.sciencemag.org/content/312/5770/117.full.html#ref-list-1>

This article has been **cited by** 242 article(s) on the ISI Web of Science

This article has been **cited by** 100 articles hosted by HighWire Press; see:

<http://www.sciencemag.org/content/312/5770/117.full.html#related-urls>

This article appears in the following **subject collections**:

Medicine, Diseases

<http://www.sciencemag.org/cgi/collection/medicine>